

# First observation of the $h_b(1P)$ and $h_b(2P)$ bottomonium states

I. Adachi,<sup>13</sup> K. Adamczyk,<sup>44</sup> H. Aihara,<sup>68</sup> K. Arinstein,<sup>2,48</sup> Y. Arita,<sup>38</sup> D. M. Asner,<sup>51</sup> T. Aso,<sup>72</sup> V. Aulchenko,<sup>2,48</sup> T. Aushev,<sup>32,24</sup> T. Aziz,<sup>63</sup> A. M. Bakich,<sup>62</sup> V. Balagura,<sup>24</sup> Y. Ban,<sup>53</sup> E. Barberio,<sup>37</sup> A. Bay,<sup>32</sup> I. Bedny,<sup>2,48</sup> M. Belhorn,<sup>5</sup> K. Belous,<sup>21</sup> V. Bhardwaj,<sup>52</sup> B. Bhuyan,<sup>16</sup> M. Bischofberger,<sup>40</sup> S. Blyth,<sup>42</sup> A. Bondar,<sup>2,48</sup> G. Bonvicini,<sup>74</sup> A. Bozek,<sup>44</sup> M. Bračko,<sup>35,25</sup> J. Brodzicka,<sup>44</sup> O. Brovchenko,<sup>27</sup> T. E. Browder,<sup>12</sup> M.-C. Chang,<sup>6</sup> P. Chang,<sup>43</sup> Y. Chao,<sup>43</sup> A. Chen,<sup>41</sup> K.-F. Chen,<sup>43</sup> P. Chen,<sup>43</sup> B. G. Cheon,<sup>11</sup> R. Chistov,<sup>24</sup> I.-S. Cho,<sup>76</sup> K. Cho,<sup>28</sup> K.-S. Choi,<sup>76</sup> S.-K. Choi,<sup>10</sup> Y. Choi,<sup>61</sup> J. Crnkovic,<sup>15</sup> J. Dalseno,<sup>36,64</sup> M. Danilov,<sup>24</sup> A. Das,<sup>63</sup> Z. Doležal,<sup>3</sup> Z. Drásal,<sup>3</sup> A. Drutskoy,<sup>5</sup> Y.-T. Duh,<sup>43</sup> W. Dungel,<sup>20</sup> D. Dutta,<sup>16</sup> S. Eidelman,<sup>2,48</sup> D. Epifanov,<sup>2,48</sup> S. Esen,<sup>5</sup> J. E. Fast,<sup>51</sup> M. Feindt,<sup>27</sup> M. Fujikawa,<sup>40</sup> V. Gaur,<sup>63</sup> N. Gabyshev,<sup>2,48</sup> A. Garmash,<sup>2,48</sup> Y. M. Goh,<sup>11</sup> B. Golob,<sup>33,25</sup> M. Grosse Perdekamp,<sup>15,56</sup> H. Guo,<sup>58</sup> H. Ha,<sup>29</sup> J. Haba,<sup>13</sup> Y. L. Han,<sup>19</sup> K. Hara,<sup>38</sup> T. Hara,<sup>13</sup> Y. Hasegawa,<sup>60</sup> K. Hayasaka,<sup>38</sup> H. Hayashii,<sup>40</sup> D. Heffernan,<sup>50</sup> T. Higuchi,<sup>13</sup> C.-T. Hoi,<sup>43</sup> Y. Horii,<sup>67</sup> Y. Hoshi,<sup>66</sup> K. Hoshina,<sup>71</sup> W.-S. Hou,<sup>43</sup> Y. B. Hsiung,<sup>43</sup> C.-L. Hsu,<sup>43</sup> H. J. Hyun,<sup>31</sup> Y. Igarashi,<sup>13</sup> T. Iijima,<sup>38</sup> M. Imamura,<sup>38</sup> K. Inami,<sup>38</sup> A. Ishikawa,<sup>57</sup> R. Itoh,<sup>13</sup> M. Iwabuchi,<sup>76</sup> M. Iwasaki,<sup>68</sup> Y. Iwasaki,<sup>13</sup> T. Iwashita,<sup>40</sup> S. Iwata,<sup>70</sup> I. Jaegle,<sup>12</sup> M. Jones,<sup>12</sup> N. J. Joshi,<sup>63</sup> T. Julius,<sup>37</sup> H. Kakuno,<sup>68</sup> J. H. Kang,<sup>76</sup> P. Kapusta,<sup>44</sup> S. U. Kataoka,<sup>39</sup> N. Katayama,<sup>13</sup> H. Kawai,<sup>4</sup> T. Kawasaki,<sup>46</sup> H. Kichimi,<sup>13</sup> C. Kiesling,<sup>36</sup> H. J. Kim,<sup>31</sup> H. O. Kim,<sup>31</sup> J. B. Kim,<sup>29</sup> J. H. Kim,<sup>28</sup> K. T. Kim,<sup>29</sup> M. J. Kim,<sup>31</sup> S. H. Kim,<sup>11</sup> S. H. Kim,<sup>29</sup> S. K. Kim,<sup>59</sup> T. Y. Kim,<sup>11</sup> Y. J. Kim,<sup>28</sup> K. Kinoshita,<sup>5</sup> B. R. Ko,<sup>29</sup> N. Kobayashi,<sup>55,69</sup> S. Koblitz,<sup>36</sup> P. Kodyš,<sup>3</sup> Y. Koga,<sup>38</sup> S. Korpar,<sup>35,25</sup> R. T. Kouzes,<sup>51</sup> M. Kreps,<sup>27</sup> P. Križan,<sup>33,25</sup> T. Kuhr,<sup>27</sup> R. Kumar,<sup>52</sup> T. Kumita,<sup>70</sup> E. Kurihara,<sup>4</sup> Y. Kuroki,<sup>50</sup> A. Kuzmin,<sup>2,48</sup> P. Kvasnička,<sup>3</sup> Y.-J. Kwon,<sup>76</sup> S.-H. Kyeong,<sup>76</sup> J. S. Lange,<sup>7</sup> I. S. Lee,<sup>11</sup> M. J. Lee,<sup>59</sup> S. E. Lee,<sup>59</sup> S.-H. Lee,<sup>29</sup> M. Leitgab,<sup>15,56</sup> R. Leitner,<sup>3</sup> J. Li,<sup>59</sup> Y. Li,<sup>73</sup> J. Libby,<sup>17</sup> C.-L. Lim,<sup>76</sup> A. Limosani,<sup>37</sup> C. Liu,<sup>58</sup> Y. Liu,<sup>43</sup> Z. Q. Liu,<sup>19</sup> D. Liventsev,<sup>24</sup> R. Louvot,<sup>32</sup> J. MacNaughton,<sup>13</sup> D. Marlow,<sup>54</sup> A. Matyja,<sup>44</sup> S. McOnie,<sup>62</sup> T. Medvedeva,<sup>24</sup> Y. Mikami,<sup>67</sup> M. Nayak,<sup>17</sup> K. Miyabayashi,<sup>40</sup> Y. Miyachi,<sup>55,75</sup> H. Miyata,<sup>46</sup> Y. Miyazaki,<sup>38</sup> R. Mizuk,<sup>24</sup> G. B. Mohanty,<sup>63</sup> D. Mohapatra,<sup>73</sup> A. Moll,<sup>36,64</sup> T. Mori,<sup>38</sup> T. Müller,<sup>27</sup> N. Muramatsu,<sup>55,50</sup> R. Mussa,<sup>23</sup> T. Nagamine,<sup>67</sup> Y. Nagasaka,<sup>14</sup> Y. Nakahama,<sup>68</sup> I. Nakamura,<sup>13</sup> E. Nakano,<sup>49</sup> T. Nakano,<sup>55,50</sup> M. Nakao,<sup>13</sup> H. Nakayama,<sup>13</sup> H. Nakazawa,<sup>41</sup> Z. Natkaniec,<sup>44</sup> E. Nedelkovska,<sup>36</sup> K. Neichi,<sup>66</sup> S. Neubauer,<sup>27</sup> C. Ng,<sup>68</sup> M. Niiyama,<sup>55,30</sup> S. Nishida,<sup>13</sup> K. Nishimura,<sup>12</sup> O. Nitoh,<sup>71</sup> S. Noguchi,<sup>40</sup> T. Nozaki,<sup>13</sup> A. Ogawa,<sup>56</sup> S. Ogawa,<sup>65</sup> T. Ohshima,<sup>38</sup> S. Okuno,<sup>26</sup> S. L. Olsen,<sup>59,12</sup> Y. Onuki,<sup>67</sup> W. Ostrowicz,<sup>44</sup> H. Ozaki,<sup>13</sup> P. Pakhlov,<sup>24</sup> G. Pakhlova,<sup>24</sup> H. Palka,<sup>44</sup> C. W. Park,<sup>61</sup> H. Park,<sup>31</sup> H. K. Park,<sup>31</sup> K. S. Park,<sup>61</sup> L. S. Peak,<sup>62</sup> T. K. Pedlar,<sup>34</sup> T. Peng,<sup>58</sup> R. Pestotnik,<sup>25</sup> M. Peters,<sup>12</sup> M. Petrič,<sup>25</sup> L. E. Piilonen,<sup>73</sup> A. Poluektov,<sup>2,48</sup> M. Prim,<sup>27</sup> K. Prothmann,<sup>36,64</sup> B. Reisert,<sup>36</sup> M. Ritter,<sup>36</sup> M. Röhrken,<sup>27</sup> J. Rorie,<sup>12</sup> M. Rozanska,<sup>44</sup> S. Ryu,<sup>59</sup> H. Sahoo,<sup>12</sup> K. Sakai,<sup>13</sup> Y. Sakai,<sup>13</sup> D. Santel,<sup>5</sup> N. Sasao,<sup>30</sup> O. Schneider,<sup>32</sup> P. Schönmeier,<sup>67</sup> C. Schwanda,<sup>20</sup> A. J. Schwartz,<sup>5</sup> R. Seidl,<sup>56</sup> A. Sekiya,<sup>40</sup> K. Senyo,<sup>38</sup> O. Seon,<sup>38</sup> M. E. Seviar,<sup>37</sup> L. Shang,<sup>19</sup> M. Shapkin,<sup>21</sup> V. Shebalin,<sup>2,48</sup> C. P. Shen,<sup>12</sup> T.-A. Shibata,<sup>55,69</sup> H. Shibuya,<sup>65</sup> S. Shinomiya,<sup>50</sup> J.-G. Shiu,<sup>43</sup> B. Shwartz,<sup>2,48</sup> F. Simon,<sup>36,64</sup> J. B. Singh,<sup>52</sup> R. Sinha,<sup>22</sup> P. Smerkol,<sup>25</sup> Y.-S. Sohn,<sup>76</sup> A. Sokolov,<sup>21</sup> E. Solovieva,<sup>24</sup> S. Stanič,<sup>47</sup> M. Starič,<sup>25</sup> J. Stypula,<sup>44</sup> S. Sugihara,<sup>68</sup> A. Sugiyama,<sup>57</sup> M. Sumihama,<sup>55,8</sup> K. Sumisawa,<sup>13</sup> T. Sumiyoshi,<sup>70</sup> K. Suzuki,<sup>38</sup> S. Suzuki,<sup>57</sup> S. Y. Suzuki,<sup>13</sup> H. Takeichi,<sup>38</sup> M. Tanaka,<sup>13</sup> S. Tanaka,<sup>13</sup> N. Taniguchi,<sup>13</sup> G. Tatishvili,<sup>51</sup> G. N. Taylor,<sup>37</sup> Y. Teramoto,<sup>49</sup> I. Tikhomirov,<sup>24</sup> K. Trabelsi,<sup>13</sup> Y. F. Tse,<sup>37</sup> T. Tsuboyama,<sup>13</sup> Y.-W. Tung,<sup>43</sup> M. Uchida,<sup>55,69</sup> T. Uchida,<sup>13</sup> Y. Uchida,<sup>9</sup> S. Uehara,<sup>13</sup> K. Ueno,<sup>43</sup> T. Uglov,<sup>24</sup> M. Ullrich,<sup>7</sup> Y. Unno,<sup>11</sup> S. Uno,<sup>13</sup> P. Urquijo,<sup>1</sup> Y. Ushiroda,<sup>13</sup> Y. Usov,<sup>2,48</sup> S. E. Vahsen,<sup>12</sup> P. Vanhoefer,<sup>36</sup> G. Varner,<sup>12</sup> K. E. Varvell,<sup>62</sup> K. Vervink,<sup>32</sup> A. Vinokurova,<sup>2,48</sup> A. Vossen,<sup>18</sup> C. H. Wang,<sup>42</sup> J. Wang,<sup>53</sup> M.-Z. Wang,<sup>43</sup> P. Wang,<sup>19</sup> X. L. Wang,<sup>19</sup> M. Watanabe,<sup>46</sup> Y. Watanabe,<sup>26</sup> R. Wedd,<sup>37</sup> M. Werner,<sup>7</sup> E. White,<sup>5</sup> J. Wicht,<sup>13</sup> L. Widhalm,<sup>20</sup> J. Wiechczynski,<sup>44</sup> K. M. Williams,<sup>73</sup> E. Won,<sup>29</sup> T.-Y. Wu,<sup>43</sup> B. D. Yabsley,<sup>62</sup> H. Yamamoto,<sup>67</sup> J. Yamaoka,<sup>12</sup> Y. Yamashita,<sup>45</sup> M. Yamauchi,<sup>13</sup> C. Z. Yuan,<sup>19</sup> Y. Yusa,<sup>73</sup> D. Zander,<sup>27</sup> C. C. Zhang,<sup>19</sup> L. M. Zhang,<sup>58</sup> Z. P. Zhang,<sup>58</sup> L. Zhao,<sup>58</sup> V. Zhilich,<sup>2,48</sup> P. Zhou,<sup>74</sup> V. Zhulanov,<sup>2,48</sup> T. Zivko,<sup>25</sup> A. Zupanc,<sup>27</sup> N. Zwahlen,<sup>32</sup> and O. Zyukova,<sup>2,48</sup>

(The Belle Collaboration)

<sup>1</sup>University of Bonn, Bonn

<sup>2</sup>Budker Institute of Nuclear Physics, Novosibirsk

<sup>3</sup>Faculty of Mathematics and Physics, Charles University, Prague

<sup>4</sup>Chiba University, Chiba

<sup>5</sup>University of Cincinnati, Cincinnati, Ohio 45221

<sup>6</sup>Department of Physics, Fu Jen Catholic University, Taipei

<sup>7</sup>Justus-Liebig-Universität Gießen, Gießen

- <sup>8</sup>Gifu University, Gifu
- <sup>9</sup>The Graduate University for Advanced Studies, Hayama
- <sup>10</sup>Gyeongsang National University, Chinju
- <sup>11</sup>Hanyang University, Seoul
- <sup>12</sup>University of Hawaii, Honolulu, Hawaii 96822
- <sup>13</sup>High Energy Accelerator Research Organization (KEK), Tsukuba
- <sup>14</sup>Hiroshima Institute of Technology, Hiroshima
- <sup>15</sup>University of Illinois at Urbana-Champaign, Urbana, Illinois 61801
- <sup>16</sup>Indian Institute of Technology Guwahati, Guwahati
- <sup>17</sup>Indian Institute of Technology Madras, Madras
- <sup>18</sup>Indiana University, Bloomington, Indiana 47408
- <sup>19</sup>Institute of High Energy Physics, Chinese Academy of Sciences, Beijing
- <sup>20</sup>Institute of High Energy Physics, Vienna
- <sup>21</sup>Institute of High Energy Physics, Protvino
- <sup>22</sup>Institute of Mathematical Sciences, Chennai
- <sup>23</sup>INFN - Sezione di Torino, Torino
- <sup>24</sup>Institute for Theoretical and Experimental Physics, Moscow
- <sup>25</sup>J. Stefan Institute, Ljubljana
- <sup>26</sup>Kanagawa University, Yokohama
- <sup>27</sup>Institut für Experimentelle Kernphysik, Karlsruher Institut für Technologie, Karlsruhe
- <sup>28</sup>Korea Institute of Science and Technology Information, Daejeon
- <sup>29</sup>Korea University, Seoul
- <sup>30</sup>Kyoto University, Kyoto
- <sup>31</sup>Kyungpook National University, Taegu
- <sup>32</sup>École Polytechnique Fédérale de Lausanne (EPFL), Lausanne
- <sup>33</sup>Faculty of Mathematics and Physics, University of Ljubljana, Ljubljana
- <sup>34</sup>Luther College, Decorah, Iowa 52101
- <sup>35</sup>University of Maribor, Maribor
- <sup>36</sup>Max-Planck-Institut für Physik, München
- <sup>37</sup>University of Melbourne, School of Physics, Victoria 3010
- <sup>38</sup>Nagoya University, Nagoya
- <sup>39</sup>Nara University of Education, Nara
- <sup>40</sup>Nara Women's University, Nara
- <sup>41</sup>National Central University, Chung-li
- <sup>42</sup>National United University, Miao Li
- <sup>43</sup>Department of Physics, National Taiwan University, Taipei
- <sup>44</sup>H. Niewodniczanski Institute of Nuclear Physics, Krakow
- <sup>45</sup>Nippon Dental University, Niigata
- <sup>46</sup>Niigata University, Niigata
- <sup>47</sup>University of Nova Gorica, Nova Gorica
- <sup>48</sup>Novosibirsk State University, Novosibirsk
- <sup>49</sup>Osaka City University, Osaka
- <sup>50</sup>Osaka University, Osaka
- <sup>51</sup>Pacific Northwest National Laboratory, Richland, Washington 99352
- <sup>52</sup>Panjab University, Chandigarh
- <sup>53</sup>Peking University, Beijing
- <sup>54</sup>Princeton University, Princeton, New Jersey 08544
- <sup>55</sup>Research Center for Nuclear Physics, Osaka
- <sup>56</sup>RIKEN BNL Research Center, Upton, New York 11973
- <sup>57</sup>Saga University, Saga
- <sup>58</sup>University of Science and Technology of China, Hefei
- <sup>59</sup>Seoul National University, Seoul
- <sup>60</sup>Shinshu University, Nagano
- <sup>61</sup>Sungkyunkwan University, Suwon
- <sup>62</sup>School of Physics, University of Sydney, NSW 2006
- <sup>63</sup>Tata Institute of Fundamental Research, Mumbai
- <sup>64</sup>Excellence Cluster Universe, Technische Universität München, Garching
- <sup>65</sup>Toho University, Funabashi
- <sup>66</sup>Tohoku Gakuin University, Tagajo
- <sup>67</sup>Tohoku University, Sendai
- <sup>68</sup>Department of Physics, University of Tokyo, Tokyo
- <sup>69</sup>Tokyo Institute of Technology, Tokyo
- <sup>70</sup>Tokyo Metropolitan University, Tokyo
- <sup>71</sup>Tokyo University of Agriculture and Technology, Tokyo

<sup>72</sup>*Toyama National College of Maritime Technology, Toyama*  
<sup>73</sup>*CNP, Virginia Polytechnic Institute and State University, Blacksburg, Virginia 24061*  
<sup>74</sup>*Wayne State University, Detroit, Michigan 48202*  
<sup>75</sup>*Yamagata University, Yamagata*  
<sup>76</sup>*Yonsei University, Seoul*  
(Dated: January 8, 2019)

We report the observation of the  $h_b(1P)$  and  $h_b(2P)$  spin-singlet bottomonium states produced in the reaction  $e^+e^- \rightarrow h_b(nP)\pi^+\pi^-$  with significances of  $5.5\sigma$  and  $11.2\sigma$ , respectively. We find that  $M[h_b(1P)] = (9898.25 \pm 1.06_{-1.07}^{+1.03}) \text{ MeV}/c^2$  and  $M[h_b(2P)] = (10259.76 \pm 0.64_{-1.03}^{+1.43}) \text{ MeV}/c^2$ , which correspond to measurements of the P-wave hyperfine splittings  $\Delta M_{\text{HF}} = (1.62 \pm 1.52) \text{ MeV}/c^2$  and  $(0.48_{-1.22}^{+1.57}) \text{ MeV}/c^2$ , respectively. We also report measurements of the cross sections for  $e^+e^- \rightarrow h_b(nP)\pi^+\pi^-$  relative to the cross section for the  $e^+e^- \rightarrow \Upsilon(2S)\pi^+\pi^-$  reaction. These results are obtained from a  $121.4 \text{ fb}^{-1}$  data sample collected with the Belle detector near the  $\Upsilon(5S)$  resonance at the KEKB asymmetric-energy  $e^+e^-$  collider.

PACS numbers: 14.40.Pq, 13.25.Gv, 12.39.Pn

Heavy quarkonium spectroscopy (the study of heavy quark-antiquark bound states, such as bottomonium ( $b\bar{b}$ )) has long been regarded as an ideal laboratory for the investigation of the interaction which governs the structure of quarkonia, Quantum Chromodynamics (QCD). Bottomonium is particularly attractive because of the very rich array of bound states below the open-flavor threshold, and because the system is nearly non-relativistic due to the large mass of the constituent quarks.

Measurements of bottomonium masses, total widths and transition rates serve as important benchmarks for the predictions of QCD-inspired potential models, non-relativistic QCD and lattice QCD [1]. In particular, the spin-singlet P-wave states of bottomonium are important as tests of the P-wave spin-spin (or hyperfine) interaction in the  $b\bar{b}$  system. The strength of this interaction is reflected in the difference between the mass of the spin-singlet state ( $h_b(nP)$  or  $n^1P_1$ ) and the weighted average of the masses of the corresponding P-wave triplet states ( $\chi_{bJ}(nP)$  or  $n^3P_J$ ). Conventionally, this difference is defined as  $\Delta M_{\text{HF}} \equiv \langle M(n^3P_J) \rangle - M(n^1P_1)$ . In charmonium, the P-wave hyperfine splitting is measured to be consistent with zero  $\Delta M_{\text{HF}} = (0.14 \pm 0.30) \text{ MeV}/c^2$  [2]. An even smaller deviation is expected in bottomonium [3]. The expected  $h_b(1P)$  and  $h_b(2P)$  widths are of the order of 100 keV [3] and are very small compared to our detector resolution.

The Belle Collaboration has collected a large sample of  $e^+e^-$  collisions at the energy of the  $\Upsilon(5S)$  resonance, which lies above the threshold for production of  $B_s$  meson pairs. The data set was collected primarily for the purpose of studying decays of  $B_s$ , but there have also been a number of unexpected observations among the non- $B_s\bar{B}_s$  decays of the  $\Upsilon(5S)$ .

Among these is the observation of anomalously large rates for dipion transitions to lower bottomonium states  $\Upsilon(5S) \rightarrow \Upsilon(nS)\pi^+\pi^-$  ( $n = 1, 2, 3$ ) [4]. If these signals are attributed entirely to the  $\Upsilon(5S)$  decays, the mea-

sured partial decay widths  $\Gamma[\Upsilon(5S) \rightarrow \Upsilon(nS)\pi^+\pi^-] \sim 0.5 \text{ MeV}$  are about two orders of magnitude larger than typical widths for dipion transitions among  $\Upsilon(nS)$  states with  $n \leq 4$ . One possible explanation is the existence, nearby in mass to the  $\Upsilon(5S)$ , of an exotic resonance  $Y_b$  which is responsible for the high transition rates [5]. The  $Y_b$  is postulated as a bottom-quark analog to the unusual charmonium-like resonance  $Y(4260)$  [6] which has an anomalously high rate of transition to  $J/\psi\pi^+\pi^-$  (much larger than the corresponding decay  $\psi' \rightarrow J/\psi\pi^+\pi^-$ ).

In an attempt to observe direct evidence for  $Y_b$  as a resonance that can be distinguished from  $\Upsilon(5S)$ , Belle collected data in a fine energy scan around the  $\Upsilon(5S)$  peak [7]. It was observed in these data that the line shape of the  $\Upsilon(nS)\pi^+\pi^-$  cross section differs from the total hadronic cross section at the  $2\sigma$  level. Larger statistics is therefore required to clarify the existence of the  $Y_b$ .

A second unexpected finding in the  $\Upsilon(5S)$  data is the observation of the decay  $\Upsilon(5S) \rightarrow \bar{B}B^*\pi$  with a branching fraction of  $(7.3_{-2.1}^{+2.3} \pm 0.8)\%$  [8], which is at least an order of magnitude higher than expectations [9].

Recently the CLEO Collaboration observed the process  $e^+e^- \rightarrow h_c(1P)\pi^+\pi^-$  at a rate comparable to the process  $e^+e^- \rightarrow J/\psi\pi^+\pi^-$  at  $\sqrt{s} = 4170 \text{ MeV}$  and found an indication of an even higher transition rate at the  $Y(4260)$  energy [10]. This implies that the  $h_b(nP)$  production might be enhanced in the region of the  $Y_b$  and motivates a search for the  $h_b(nP)$  in the  $\Upsilon(5S)$  data.

In this article, we report the first observation of the  $h_b(1P)$  and  $h_b(2P)$  produced via  $e^+e^- \rightarrow h_b(nP)\pi^+\pi^-$  in the  $\Upsilon(5S)$  region. We use the full data sample corresponding to an integrated luminosity of  $121.4 \text{ fb}^{-1}$  collected near the peak of the  $\Upsilon(5S)$  resonance ( $\sqrt{s} \sim 10.865 \text{ GeV}$ ) with the Belle detector at the KEKB asymmetric  $e^+e^-$  collider [11].

The Belle detector is a large-solid-angle magnetic spectrometer that consists of a 4-layer silicon vertex detector (SVD), a 50-layer central drift chamber (CDC), an array of aerogel threshold Cherenkov counters (ACC),

a barrel-like arrangement of time-of-flight scintillation counters (TOF), and an electromagnetic calorimeter (ECL) of CsI(Tl) crystals located inside a superconducting solenoid coil that provides a 1.5 T magnetic field. An iron flux-return located outside of the coil is instrumented to detect  $K_L^0$  mesons and to identify muons (KLM). The detector is described in detail elsewhere [12].

We use a GEANT-based Monte Carlo (MC) simulation [13] to model the response of the detector and determine the acceptance. The MC simulation includes run-dependent detector performance variations and background conditions.

We observe  $h_b(1P)$  and  $h_b(2P)$  in the missing mass spectrum of  $\pi^+\pi^-$  pairs. The  $\pi^+\pi^-$  missing mass is defined as

$$MM(\pi^+\pi^-) \equiv \sqrt{(E_{c.m.} - E_{\pi^+\pi^-}^*)^2 - p_{\pi^+\pi^-}^{*2}},$$

where  $E_{c.m.}$  is the center-of-mass (c.m.) energy,  $E_{\pi^+\pi^-}^*$  and  $p_{\pi^+\pi^-}^*$  are the  $\pi^+\pi^-$  energy and momentum measured in the c.m. frame.

Hadronic events are initially selected by requiring at least three reconstructed charged tracks, a total reconstructed ECL energy in the c.m. in the range  $(0.1 - 0.8)E_{c.m.}$ , at least one large-angle cluster in the ECL, a total visible energy - calculated from all charged tracks and isolated neutral showers - greater than  $0.2E_{c.m.}$ , the absolute value of the z component of the c.m. momentum less than  $0.5E_{c.m.}$ , and a reconstructed primary vertex that is consistent with the known location of the run-averaged interaction point (IP).

We select high-quality tracks that originate from the vicinity of the IP. We require that the tracks are positively identified as pions based on the CDC (dE/dx), TOF and ACC information; and we reject well identified electrons. The continuum  $e^+e^- \rightarrow q\bar{q}$  ( $q = u, d, s, c$ ) background is suppressed by a requirement that the ratio of the second to zeroth Fox-Wolfram moments satisfy  $R_2 < 0.3$  [14]. These selection requirements are optimized by maximizing the significance of the high statistics calibration channel  $\Upsilon(5S) \rightarrow \Upsilon(2S)\pi^+\pi^-$ .

The  $MM(\pi^+\pi^-)$  distribution for the selected  $\pi^+\pi^-$  pairs is shown in Fig. 1. The signals are difficult to see in this figure because of very high combinatorial background. We will determine yields for various  $\pi^+\pi^-$  transitions by fitting this spectrum to a background function plus signal shapes for the desired  $\pi^+\pi^-$  transitions.

To determine appropriate signal shapes we fully reconstruct exclusive transitions  $\Upsilon(5S) \rightarrow \pi^+\pi^-\Upsilon(nS) \rightarrow \pi^+\pi^-\mu^+\mu^-$ . We use the same selection requirements for muons as in Ref. [4]. Muons are identified by their range and transverse scattering in the KLM and are required to originate from the vicinity of the IP. The  $\pi^+\pi^-$  selection is identical to the inclusive case. To suppress the background process  $e^+e^- \rightarrow \mu^+\mu^-\gamma \rightarrow \mu^+\mu^-e^+e^-$  in which the electrons are misidentified as pions, we require the opening angle between the pions to satisfy

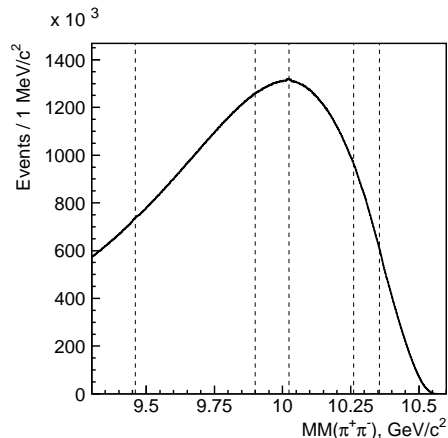


FIG. 1: The  $MM(\pi^+\pi^-)$  distribution for the selected  $\pi^+\pi^-$  pairs. Vertical lines indicate the locations of the  $\Upsilon(1S)$ ,  $h_b(1P)$ ,  $\Upsilon(2S)$ ,  $h_b(2P)$  and  $\Upsilon(3S)$  signals.

$\cos\theta_{\pi^+\pi^-} < 0.95$ . The two-dimensional distribution of  $\mu^+\mu^-$  mass  $M(\mu^+\mu^-)$  vs.  $MM(\pi^+\pi^-)$  shows many structures, as presented in Fig. 2 (a). This plot is very similar to the plot  $M(\mu^+\mu^-)$  vs.  $M(\pi^+\pi^-\mu^+\mu^-) - M(\pi^+\pi^-)$  that appears in Ref. [4] because the quantities  $M(\pi^+\pi^-\mu^+\mu^-) - M(\pi^+\pi^-)$  and  $MM(\pi^+\pi^-)$  are tightly correlated.

To study the signals of exclusively reconstructed decay chains  $\Upsilon(5S) \rightarrow \Upsilon(nS)\pi^+\pi^- \rightarrow \mu^+\mu^-\pi^+\pi^-$  we require that  $|MM(\pi^+\pi^-) - M(\mu^+\mu^-)| < 150 \text{ MeV}/c^2$ . The corresponding  $MM(\pi^+\pi^-)$  distributions in the regions of the  $\Upsilon(1S)$ ,  $\Upsilon(2S)$  and  $\Upsilon(3S)$  are shown in Figs. 2 (b)-(d). The high-mass tails of the signals are attributed to initial state radiation (ISR) of low energy photons. The MC simulation of the ISR process, which takes into account the energy dependence of the cross-section [7], is consistent with data. We fit each  $MM(\pi^+\pi^-)$  distribution for these direct transitions to a sum of a Crystal Ball function describing the signal and a first-order polynomial describing the background. The fit results are shown in Figs. 2 (b)-(d) and in Table I. Here and throughout the

TABLE I: The yield, mass and width for signals reconstructed in the  $\mu^+\mu^-\pi^+\pi^-$  final state.

	Yield	Mass, $\text{MeV}/c^2$	$\sigma$ , $\text{MeV}/c^2$
$\Upsilon(1S)$	$1868 \pm 57$	$9459.96 \pm 0.23$	$7.49 \pm 0.21$
$\Upsilon(2S)$	$2300 \pm 59$	$10023.32 \pm 0.19$	$6.50 \pm 0.17$
$\Upsilon(3S)$	$607 \pm 29$	$10355.66 \pm 0.39$	$5.68 \pm 0.38$
$3S \rightarrow 1S$	$684 \pm 36$	$9973.01 \pm 0.98$	$17.54 \pm 0.90$
$2S \rightarrow 1S$	$2618 \pm 57$	$10303.93 \pm 0.26$	$11.49 \pm 0.23$

paper the first uncertainty is statistical and the second, if present, is systematic (unless mentioned otherwise). The high-mass tails of these peaks contain roughly 8% of the

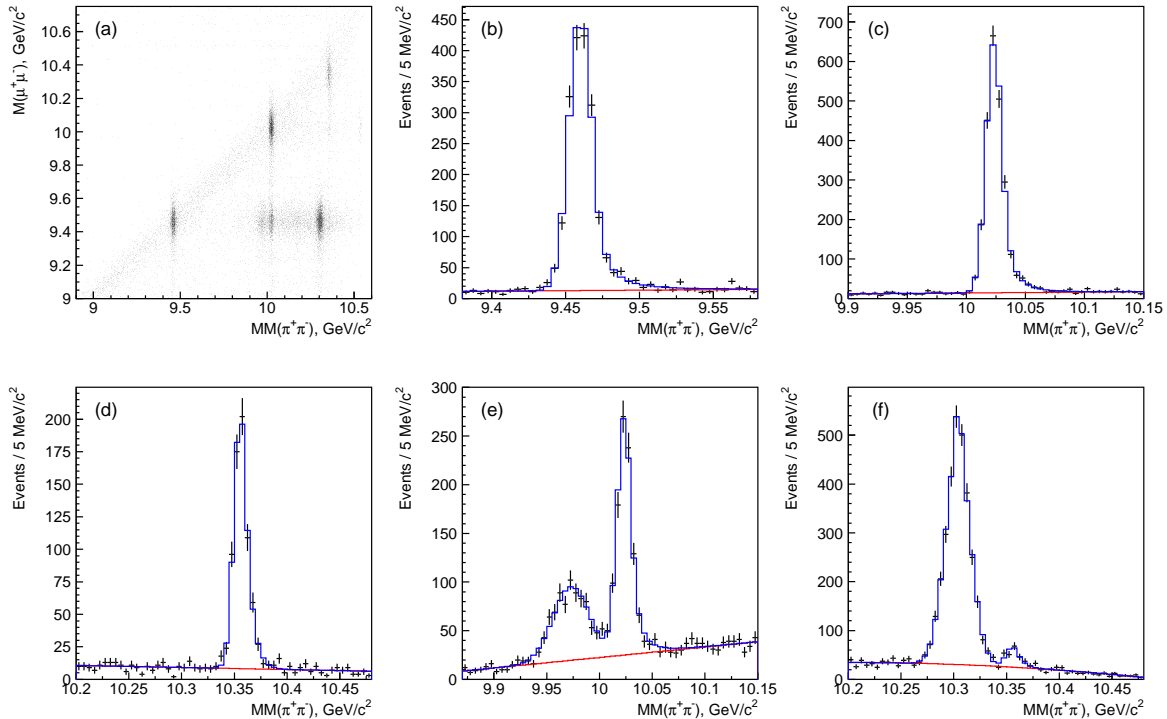


FIG. 2: (a) Distribution  $M(\mu^+\mu^-)$  vs.  $MM(\pi^+\pi^-)$ , and its projection on  $MM(\pi^+\pi^-)$  for the slanted band  $|MM(\pi^+\pi^-) - M(\mu^+\mu^-)| < 150 \text{ MeV}/c^2$  in the regions of the  $\Upsilon(1S)$ ,  $\Upsilon(2S)$  and  $\Upsilon(3S)$  [(b) to (d)]; and for the horizontal band  $|M(\mu^+\mu^-) - M[\Upsilon(1S)]| < 150 \text{ MeV}/c^2$  in the regions of the  $\Upsilon(2S)$  and  $\Upsilon(3S)$  [(e) and (f)].

yield.

In order to study the remaining structures seen in Fig. 2 (a), we require  $|M(\mu^+\mu^-) - M(\Upsilon(1S))| < 150 \text{ MeV}/c^2$ . In Figs. 2 (e)-(f) we present the corresponding  $MM(\pi^+\pi^-)$  projection for the regions near the  $\Upsilon(2S)$  and  $\Upsilon(3S)$ . The peaks centered at  $9.97 \text{ GeV}/c^2$  and  $10.30 \text{ GeV}/c^2$  correspond to transitions  $\Upsilon(3S) \rightarrow \Upsilon(1S)\pi^+\pi^-$  and  $\Upsilon(2S) \rightarrow \Upsilon(1S)\pi^+\pi^-$ , respectively, where  $\Upsilon(3S)$  and  $\Upsilon(2S)$  are produced either inclusively in the  $\Upsilon(5S)$  decays or via ISR processes, with the subsequent decay of the daughter  $\Upsilon(1S) \rightarrow \mu^+\mu^-$ . These two peaks are described by single and double Gaussians, respectively. The parameters are shown in Table I. The Figs. 2 (e)-(f) also show peaks at the nominal  $\Upsilon(2S)$  and  $\Upsilon(3S)$  masses, which correspond to direct transitions  $\Upsilon(5S) \rightarrow (\Upsilon(2S), \Upsilon(3S))\pi^+\pi^-$  with subsequent inclusive decay of these resonances to  $\Upsilon(1S)$ , with  $\Upsilon(1S)$  decaying to  $\mu^+\mu^-$ . The yields of these signals are found to be  $869 \pm 34$  and  $144 \pm 17$ , respectively.

The measured masses do not show significant deviations from PDG [2] values. The resolution in data as compared to MC simulation is found to be worse by factors of  $1.16 \pm 0.03$ ,  $1.14 \pm 0.03$  and  $1.07 \pm 0.06$  for the  $\Upsilon(1S)$ ,  $\Upsilon(2S)$  and  $\Upsilon(3S)$ , respectively. According to the MC simulation, there is no difference in the  $MM(\pi^+\pi^-)$  peak position and resolution for exclusive and inclusive

reconstruction of the  $\Upsilon(nS)$ . Therefore we use the signal shapes determined from exclusive data to fit the inclusive data.

An additional background which must be accounted for arises due to the existence of the kinematic threshold for the inclusive production of  $K_S^0$  in  $\Upsilon(5S)$  decay. The inclusively produced  $K_S^0 \rightarrow \pi^+\pi^-$  contribution has a rapid rise above the threshold in  $MM(\pi^+\pi^-)$ , as shown in Fig. 3. We notice that the position of this rapid rise is

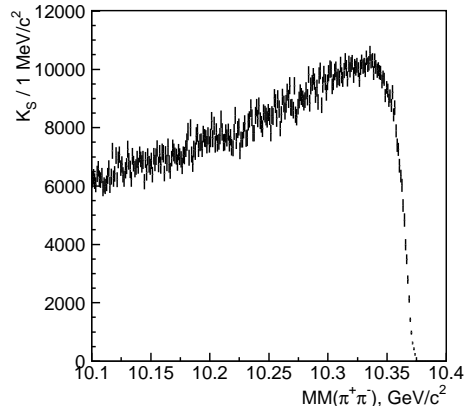


FIG. 3: The  $K_S^0$  yield as a function of the  $MM(\pi^+\pi^-)$ .

close to the  $\Upsilon(3S)$  signal. The yields of  $K_S^0 \rightarrow \pi^+\pi^-$  in Fig. 3 are determined from fits to the  $M(\pi^+\pi^-)$  spectra in  $MM(\pi^+\pi^-)$  bins. The  $K_S^0$  signal is described by a Gaussian, while for the background we use an ARGUS function convolved with a Gaussian. The cut-off of the ARGUS function is fixed for every  $MM(\pi^+\pi^-)$  bin to  $10.865 \text{ GeV}/c^2 - MM(\pi^+\pi^-)$ . The width of the Gaussian with which the ARGUS function is convolved is determined from the fit to the  $M(\pi^+\pi^-)$  spectrum in about  $20 \text{ MeV}/c^2$  wide  $MM(\pi^+\pi^-)$  interval and then is fixed for every  $1 \text{ MeV}/c^2$  wide  $MM(\pi^+\pi^-)$  bin. The dependence of the  $K_S^0$  peak position and width on  $MM(\pi^+\pi^-)$  agrees qualitatively with generic MC expectations.

To fit the  $MM(\pi^+\pi^-)$  spectrum, we separate it into three adjacent regions with boundaries at  $MM(\pi^+\pi^-) = 9.3 \text{ GeV}/c^2$ ,  $9.8 \text{ GeV}/c^2$ ,  $10.1 \text{ GeV}/c^2$  and  $10.45 \text{ GeV}/c^2$ . We fit every region separately to better control the complicated shape of the combinatorial background, which is described by a Chebyshev polynomial. We select the order of the polynomial that maximizes the confidence level of the fit. For regions 1 and 2 we use a 6th-order polynomial while for region 3 we use a 7th-order polynomial. In region 3 we subtract the  $K_S^0$  contribution bin-by-bin, while in other regions its shape is smooth and is absorbed into combinatorial background. The signal component of the fit function includes all signals seen in the  $\mu^+\mu^-\pi^+\pi^-$  data and the  $h_b(1P)$ ,  $h_b(2P)$  and  $\Upsilon(1D)$ . The tail parameters of the additional signals are assumed to be the same as for the  $\Upsilon(2S)$ , while the widths are found by linear interpolation in mass. The peak positions of all signals are floated, except the position of the  $\Upsilon(3S) \rightarrow \Upsilon(1S)\pi^+\pi^-$  signal which is poorly constrained by the fit.

We perform binned  $\chi^2$  fits to each region using  $1 \text{ MeV}/c^2$  bins, though for clarity we display the data in  $5 \text{ MeV}/c^2$  bins. The  $MM(\pi^+\pi^-)$  spectrum with the combinatorial background and  $K_S^0$  contributions subtracted, and the signal function resulting from the fit overlaid, is shown in Fig. 4. The fit results for the yields, peak positions and statistical significances are shown in Table II. The confidence levels of the fits are 3%, 0.5%

TABLE II: The yield, mass and statistical significance from the fits to the missing mass distributions of inclusive  $\pi^+\pi^-$  pairs.

	Yield, $10^3$	Mass, $\text{MeV}/c^2$	Signif., $\sigma$
$\Upsilon(1S)$	$105.2 \pm 5.8 \pm 3.0$	$9459.42 \pm 0.53 \pm 1.02$	18.2
$h_b(1P)$	$50.4 \pm 7.8_{-9.1}^{+4.5}$	$9898.25 \pm 1.06_{-1.07}^{+1.03}$	6.2
$3S \rightarrow 1S$	$55 \pm 19$	9973.01	2.9
$\Upsilon(2S)$	$143.4 \pm 8.7 \pm 6.8$	$10022.25 \pm 0.41 \pm 1.01$	16.6
$\Upsilon(1D)$	$22.1 \pm 7.8$	$10166.2 \pm 2.4$	2.4
$h_b(2P)$	$84.4 \pm 6.8_{-10.0}^{+23.0}$	$10259.76 \pm 0.64_{-1.03}^{+1.43}$	12.4
$2S \rightarrow 1S$	$151.6 \pm 9.7_{-20.0}^{+9.0}$	$10304.57 \pm 0.61 \pm 1.03$	15.7
$\Upsilon(3S)$	$44.9 \pm 5.1 \pm 5.1$	$10356.56 \pm 0.87 \pm 1.06$	8.5

and 0.3% for three regions, respectively. The significance for every signal is estimated from the  $\chi^2$  difference of the best fit and of the fit without the signal under study taking into account the change in the number of degrees of freedom. The statistical significance of the  $h_b(1P)$  and  $h_b(2P)$  is found to be  $6.2\sigma$  and  $12.4\sigma$ , respectively.

We have studied several sources of systematic uncertainty. (1) To estimate the uncertainty that arises from our choice of combinatorial background parameterization, we increase the polynomial order by one, two and three relative to the nominal value. While the correct estimation of the combinatorial background shape is crucial, we find that the fit results are very stable relative to these variations. (2) We vary the boundaries of the  $MM(\pi^+\pi^-)$  fit interval by a typical range of  $100 \text{ MeV}/c^2$ . (3) We have estimated the systematic uncertainty arising from the choice of the signal shape. (a) We consider the possibility that the  $h_b(1P)$  and  $h_b(2P)$  signals do not have the high-mass tails and for both with- and without-tail cases we allow the width parameter to float freely in the fit. (b) We multiply the widths of the  $\Upsilon(1S)$ ,  $\Upsilon(2S)$  and  $\Upsilon(3S)$  by a parameter and allow this parameter to float in the fit. We find for this parameter on average  $1.04 \pm 0.05$ , consistent with unity. For each fit, we increase the width of the  $h_b(1P)$  and  $h_b(2P)$  by this factor. (c) We allow the width of the  $\Upsilon(2S) \rightarrow \Upsilon(1S)\pi^+\pi^-$  signal to float in the fit. (4) We have also studied systematic uncertainties arising from our particular selection criteria. We consider the following variations: (a) We studied the effect of tightening the requirements on the  $\pi^+\pi^-$  track parameters corresponding to the point of origin - that they must originate within a tighter window around the IP. We find that these changes reduce the  $K_S^0$  yield by a factor of 1.5. (Therefore this variation tests also the systematics in the  $K_S^0$  extraction.) (b) We have introduced an additional requirement that the number of tracks in the event be greater than four. (c) We studied the effect of requiring that the opening angle between two pions in the laboratory frame satisfy  $\cos\theta_{\pi^+\pi^-} < 0.95$  (this requirement is used for  $\mu^+\mu^-\pi^+\pi^-$  data).

For each source, we assign the systematic uncertainty to be the maximal change of signal parameters that arise from the variations outlined above (see Table III). Finally, we find about  $1 \text{ MeV}/c^2$  scattering of the  $\Upsilon(1S)$ ,  $\Upsilon(2S)$  and  $\Upsilon(3S)$  peak positions relative to the PDG values. These deviations could be due to the local variations of the background shape that are not described by the polynomial in all details. Consequently, we add an additional uncertainty of  $1 \text{ MeV}/c^2$  to all mass measurements. All systematic uncertainty contributions for each quantity have been added in quadrature to obtain the total systematic uncertainty, which is shown in Table II. The significances of the  $h_b(1P)$  and  $h_b(2P)$  signals including both statistical and systematic uncertainties are  $5.5\sigma$  and  $11.2\sigma$ , respectively.

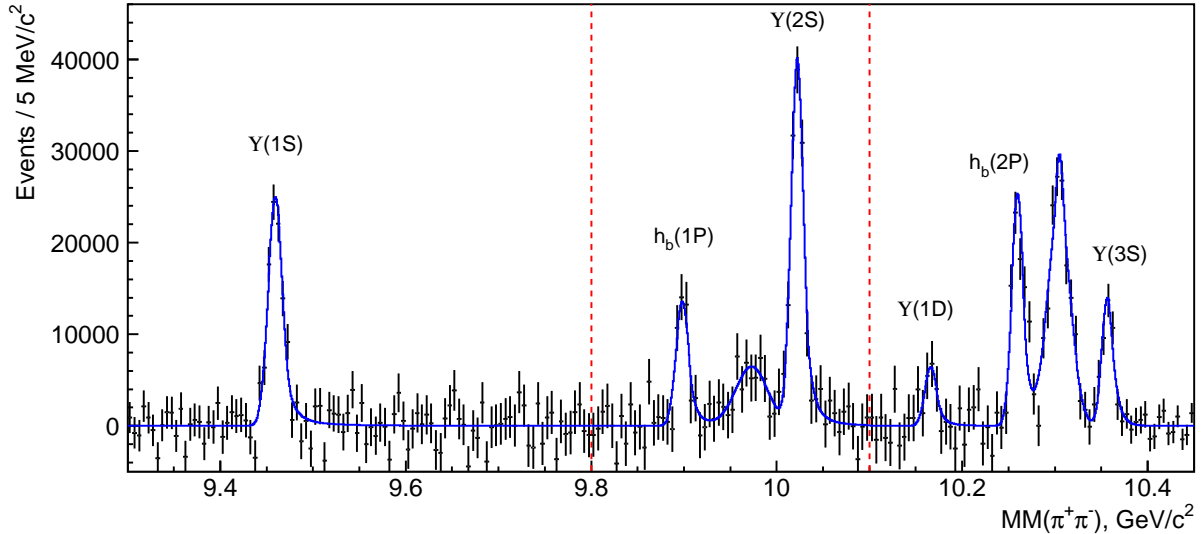


FIG. 4: The  $MM(\pi^+\pi^-)$  spectrum with the combinatorial background and  $K_S^0$  contributions subtracted (dots with error bars) and signal component of the fit function (solid histogram). The vertical dashed lines indicate the boundaries of the fit regions. The peaks centered at  $9.97 \text{ GeV}/c^2$  and  $10.30 \text{ GeV}/c^2$  correspond to transitions  $\Upsilon(3S) \rightarrow \Upsilon(1S)\pi^+\pi^-$  and  $\Upsilon(2S) \rightarrow \Upsilon(1S)\pi^+\pi^-$ , respectively (see text).

TABLE III: Absolute systematic uncertainties in the yields and masses from various sources. The units for the entries in this table appear in the left-hand column.

	Polynomial order	Fit range	Signal shape	Selection requirements
$N[\Upsilon(1S)], 10^3$	$\pm 1.4$	$\pm 1.7$	$\pm 2.0$	–
$M[\Upsilon(1S)], \text{MeV}/c^2$	$\pm 0.04$	$\pm 0.06$	$\pm 0.03$	$\pm 0.18$
$N[h_b(1P)], 10^3$	$\pm 2.4$	$\pm 3.6$	$^{+1.2}_{-8.0}$	–
$M[h_b(1P)], \text{MeV}/c^2$	$\pm 0.04$	$\pm 0.10$	$^{+0.04}_{-0.20}$	$^{+0.20}_{-0.30}$
$N[\Upsilon(2S)], 10^3$	$\pm 3.4$	$\pm 3.2$	$\pm 5.0$	–
$M[\Upsilon(2S)], \text{MeV}/c^2$	$\pm 0.02$	$\pm 0.08$	$\pm 0.06$	$\pm 0.03$
$N[h_b(2P)], 10^3$	$\pm 2.2$	$\pm 2.6$	$^{+23.}_{-9.0}$	–
$M[h_b(2P)], \text{MeV}/c^2$	$\pm 0.10$	$\pm 0.20$	$^{+1.0}_{-0.0}$	$\pm 0.08$
$N[2 \rightarrow 1], 10^3$	$\pm 3.0$	$\pm 8.0$	$^{+0}_{-18}$	–
$M[2 \rightarrow 1], \text{MeV}/c^2$	$\pm 0.20$	$\pm 0.10$	$\pm 0.06$	$\pm 0.10$
$N[\Upsilon(3S)], 10^3$	$\pm 1.0$	$\pm 3.0$	$\pm 4.0$	–
$M[\Upsilon(3S)], \text{MeV}/c^2$	$\pm 0.15$	$\pm 0.24$	$\pm 0.10$	$\pm 0.20$

Based on the yields and efficiencies we determine the ratio of production cross sections

$$\frac{\sigma(e^+e^- \rightarrow X\pi^+\pi^-)}{\sigma(e^+e^- \rightarrow \Upsilon(2S)\pi^+\pi^-)}$$

where  $X = \Upsilon(1S), \Upsilon(3S), h_b(1P)$  and  $h_b(2P)$ .

To determine the reconstruction efficiency, we calibrate the MC simulation. We begin with phase-space generated events, and apply weighting factors that are determined based on the two-dimensional distribution of

$M(\pi^+\pi^-)$  vs.  $\cos\theta_{\text{Hel}}$  in the exclusive  $\mu^+\mu^-\pi^+\pi^-$  data. Here  $\theta_{\text{Hel}}$  is the angle between  $\pi^-$  and  $\Upsilon(5S)$  momenta in the  $\pi^+\pi^-$  rest frame. To simulate the  $h_b(1P)\pi^+\pi^-$  and  $h_b(2P)\pi^+\pi^-$  final states we use weighting factors of the closest  $\Upsilon(nS)$ , the  $\Upsilon(2S)$  for the  $h_b(1P)$  and the  $\Upsilon(3S)$  for the  $h_b(2P)$ . We also use phase-space events and weights for the other  $\Upsilon(nS)$  states to determine the systematic uncertainty.

We determine the efficiency of the  $R_2 < 0.3$  requirement from data by measuring the signal yields for  $R_2 > 0.3$ .

The reconstruction efficiencies, the efficiency of the  $R_2 < 0.3$  requirement and the cross-section ratios are shown in Table IV. The uncertainty in the efficiencies is

TABLE IV: Reconstruction efficiency, efficiency of the  $R_2 < 0.3$  requirement and the ratios of cross sections relative to that for  $\Upsilon(2S)$  production.

	Reconstruction Efficiency	Efficiency $R_2 < 0.3$	Cross section relative to $e^+e^- \rightarrow \Upsilon(2S)\pi^+\pi^-$
$\Upsilon(1S)$	$0.697 \pm 0.001$	$0.855 \pm 0.040$	$0.638 \pm 0.065^{+0.037}_{-0.056}$
$\Upsilon(2S)$	$0.601 \pm 0.001$	$0.863 \pm 0.032$	1
$\Upsilon(3S)$	$0.427 \pm 0.001$	$0.736 \pm 0.063$	$0.517 \pm 0.082 \pm 0.070$
$h_b(1P)$	$0.620 \pm 0.010$	$0.723 \pm 0.068$	$0.407 \pm 0.079^{+0.043}_{-0.076}$
$h_b(2P)$	$0.490 \pm 0.015$	$0.796 \pm 0.043$	$0.78 \pm 0.09^{+0.22}_{-0.10}$

due to variations in the production models and limited MC statistics. The systematic uncertainties in the ratios include the systematic uncertainties in the signal yields

and efficiencies.

We have also used the data collected at the  $\Upsilon(4S)$  resonance to search for  $h_b(1P)$  ( $h_b(2P)$  is kinematically forbidden in  $e^+e^- \rightarrow h_b(2P)\pi^+\pi^-$  at  $\Upsilon(4S)$  energy). The integrated luminosity used for this study is  $711 \text{ fb}^{-1}$ . We do not find a statistically significant  $h_b(1P)$  signal. The yield obtained is  $(34 \pm 20) \times 10^3$ , while the reconstruction efficiency is  $0.507 \pm 0.013$ . We set upper limits on the ratio of cross sections  $\sigma(e^+e^- \rightarrow h_b(1P)\pi^+\pi^-)$  at the  $\Upsilon(4S)$  and  $\Upsilon(5S)$  energies  $R(4/5) < 0.28$  at 90% C.L.

Recently the BaBar Collaboration reported  $3.0\sigma$  evidence for the process  $\Upsilon(3S) \rightarrow h_b(1P)\pi^0$  with  $h_b(1P) \rightarrow \eta_b\gamma$  [15]. They also obtained an upper limit for the rate of the more directly comparable process,  $\Upsilon(3S) \rightarrow h_b(1P)\pi^+\pi^-$  [16]. The rate for  $e^+e^- \rightarrow h_b(nP)\pi^+\pi^-$  production that we have observed in the  $\Upsilon(5S)$  region is found to be much larger than their upper limit for the rate at  $\Upsilon(3S)$ . This is consistent with our previous observation that the rates for production of  $\Upsilon(mS)\pi^+\pi^-$  with  $m = 1, 2, 3$  at  $\Upsilon(5S)$  are much larger than the rates for  $\Upsilon(nS) \rightarrow \Upsilon(mS)\pi^+\pi^-$  for  $n \leq 4$  [4].

In summary, we have observed the  $h_b(1P)$  and  $h_b(2P)$  P-wave spin-singlet bottomonium states in the reaction  $e^+e^- \rightarrow h_b(nP)\pi^+\pi^-$  at an energy corresponding to  $\Upsilon(5S)$ . We measure the masses and the cross sections relative to the  $e^+e^- \rightarrow \Upsilon(2S)\pi^+\pi^-$  cross-section:  $M = (9898.25 \pm 1.06^{+1.03}_{-1.07}) \text{ MeV}/c^2$ ,  $R = 0.407 \pm 0.079^{+0.043}_{-0.076}$  for the  $h_b(1P)$  and  $M = (10259.76 \pm 0.64^{+1.43}_{-1.03}) \text{ MeV}/c^2$ ,  $R = 0.78 \pm 0.09^{+0.22}_{-0.10}$  for the  $h_b(2P)$ . The masses do not differ significantly from the center-of-gravity of the corresponding  $\chi_{bJ}$  states. For the hyperfine splitting we find  $\Delta M_{\text{HF}} = 1.62 \pm 1.52 \text{ MeV}/c^2$  for the  $h_b(1P)$  and  $0.48^{+1.57}_{-1.22} \text{ MeV}/c^2$  for the  $h_b(2P)$ . Here the statistical and systematic uncertainties are added in quadrature. The values of  $R$  comparable with unity indicate that the  $h_b(1P)$  and  $h_b(2P)$  are produced via an exotic process that violates the suppression of heavy quark spin-flip.

We thank the KEKB group for excellent operation of the accelerator, the KEK cryogenics group for effi-

cient solenoid operations, and the KEK computer group and the NII for valuable computing and SINET3 network support. We acknowledge support from MEXT, JSPS and Nagoya's TLPRC (Japan); ARC and DIISR (Australia); NSFC (China); MSMT (Czechia); DST (India); MEST, NRF, NSDC of KISTI, and WCU (Korea); MNiSW (Poland); MES and RFAAE (Russia); ARRS (Slovenia); SNSF (Switzerland); NSC and MOE (Taiwan); and DOE and NSF (USA).

- 
- [1] N. Brambilla *et al.*, Eur.Phys.J.C **71**, 1534 (2011).
  - [2] K. Nakamura *et al.* (Particle Data Group), J. Phys. G **37**, 075021 (2010).
  - [3] S. Godfrey and J. L. Rosner, Phys. Rev. D **66**, 014012 (2002).
  - [4] K.-F. Chen *et al.* (Belle Collaboration), Phys. Rev. Lett. **100**, 112001 (2008).
  - [5] W.-S. Hou, Phys. Rev. D **74**, 017504 (2006).
  - [6] B. Aubert *et al.* (BABAR Collaboration), Phys. Rev. Lett. **95**, 142001 (2005).
  - [7] K.-F. Chen *et al.* (Belle Collaboration), Phys. Rev. D **82**, 091106 (2010).
  - [8] A. Drutskoy *et al.* (Belle Collaboration), Phys. Rev. D **81**, 112003 (2010).
  - [9] L. Lellouch *et al.*, Nucl. Phys. B **405**, 55 (1993); Yu. Simonov *et al.*, JETP Lett. **88**, 5 (2008).
  - [10] R.E. Mitchell, arXiv:1102.3424v1.
  - [11] S. Kurokawa and E. Kikutani, Nucl. Instrum. Methods Phys. Res. Sect., A **499**, 1 (2003), and other papers included in this Volume.
  - [12] A. Abashian *et al.* (Belle Collaboration), Nucl. Instrum. Methods Phys. Res., Sect. A **479**, 117 (2002).
  - [13] R. Brun *et al.*, GEANT 3.21, CERN DD/EE/84-1, 1984.
  - [14] G.C. Fox and S. Wolfram, Phys. Rev. Lett. **41**, 1581 (1978).
  - [15] J. P. Lees *et al.* (BaBar Collaboration), arXiv:1102.4565.
  - [16] B. Fulsom (BaBar Collaboration), PoS(ICHEP 2010) 199.